[redacted]

UNCLASSIFIED

Classification Changed to UNCLASSIFIED by Authority of W H Emslie DOE SR By CTS Date 6-23-81

DPSP 55-25-38

This document consists of 45 pages. No. 22 of 36 copies, Series A.

THERMAL SHIELD AND REACTOR STRUCTURE TEMPERATURES

A. R. Collier

May 1955

RESTRICTED DATA

This document contains Restricted Data as defined in the Atomic Energy Act of 1954. Its transmittal or the disclosure in any manner of its contents to an unauthorized person is prohibited.

E. I. du Pont de Nemours and Company
Explosives Department - Atomic Energy Division
Savannah River Plant

UNCLASSIFIED

[redacted]

[redacted]

This document was prepared in conjunction with work accomplished under Contract No. AT(07-2)-1 with the U.S. Department of Energy.

DISCLAIMER

[redacted]

Distribution

Wilmington

1 J. E. Cole
2 M. H. Smith
3 H. Worthington
4 J. B. Tinker
5-6 H. W. Bellas
7 D. F. Babcock
8 J. G. Brewer, Eng Dept
9 T. H. Davis, Eng Dept
10 H. J. Kamack, Eng Dept
11 M. T. Cichelli, Eng Res Lab
12 W File

Savannah River Plant

13 D. A. Miller
14 W. P. Overbeck
15 F. H. Endorf
16 K. W. French
17 C. W. J. Wende
18 A. A. Johnson
19 P. A. Dahlen
20 E. C. Bertsche
21 D. R. Leader
22 M. S. Brinn
23 E. C. Nelson
24 J. W. Walker
25 J. T. Carlton
26 A. R. Collier
27 J. A. Monier
30 TIS File
31 TPO File
32-35 PRD File, Extra Copies
36 PRD File, Record Copy

Atomic Energy Comission, SROO

28 R. C. Blair
29 H. L. Kilburn

[redacted]

Contents

ABSTRACT

Savannah River Plant reactor structure and shield temperature measurements obtained during P-3 power ascension are compared with design calculations. Comparison shows that design calculations are conservative. Heat generation data from P-5 cycle are also presented. A ± 2°C error may exist in all the reported data.

[redacted]

Introduction

Miscellaneous center section temperatures have been measured in all Savannah River Plant 100 Areas by the Reactor Technology Section's Engineering Studies group. The data collected were never compared to design calculations. The purpose of this report is to present reactor structure and thermal shield temperature data taken during P-3 and P-5 cycles, and compare them with design calculations in order to predict temperatures at higher power levels.

Summary

Reactor structure and shield temperatures were measured at each step of the P-3 power ascension, and were compared with design calculations. Heat generation data taken in the P-5 cycle are also given.

Data and curves representing the work done appear in the appendix. The more important findings obtained from this study follow.

	Reactor Data	Design Calculations
1. Thermal Shield Maximum Wall to Wall ΔT, Metal Temperature Difference at 700 MW, °C	12.0	15.4
2. Film Coefficient From Thermal Shield Inner Wall to Shield Coolant, Pcu/hr/ft^2/°C	150	108
3. Total Reactor Heat Removed by Thermal Shield Coolant at 700 MW, %	0.178 to 0.183 extrapolated (P-3 & P-5 data)	0.5 to 0.63

Comparison of the measured structure temperatures and the design values has shown that design calculations were conservative in all cases; ie, the measured temperature differentials producing stresses are lower than the design differentials.

The reactor data presented should not be considered as completely accurate. Where absolute temperature values are concerned, an error of ± 2°C may exist even after all allowable corrections have been made. However, where temperature differentials are concerned, the percent error may be larger.

[redacted]

Recommendations

- The extrapolated curves presented in this report should be used in predicting reactor temperatures at higher power levels.
- Reactor structure temperatures should be measured with the three 16-point potentiometer recorders.
- The miscellaneous temperature recorders should be re-ranged from 0-200°C to 0-100°C, the chart speed should be advanced to 4 inches/minute (to print each point separately), and the recorders should be calibrated frequently.
- The miscellaneous temperature panel telephone jacks and plugs should be cleaned periodically to removed caked dirt and film.

Discussion

A stress analysis and limited temperature study was completed for R reactor based on R-1 data (0 to 200 MW operation). The results of the R-1 study are presented in DPSP 54-25-38. The bulk of the data is concerned with stress and motion measurement. However, where temperatures have been plotted and extrapolated to higher powers, they have been compared with the data obtained for this report. The two sets of data are not in agreement; an explanation for the difference is given in the succeeding pages.

In analyzing reactor structure temperatures above 200 MW, it was decided to continue the study in P reactor rather than R reactor for the following reasons:

- P reactor is operating at higher powers.
- Many of the thermocouples in R reactor are defective because they were wetted before being slipped into their sheaths. This wetting led to subsequent corrosion of the thermocouple wire.
- All the annular shield thermocouples are clipped on the grid blocks in R reactor, while in P reactor some couples are padded to the water side of the shield inner wall. The padded thermocouples measure the wall surface temperature, but do not give the average metal temperature. However, the latter is simply calculated if heat generation and longitudinal flux distribution data are also measured.

The majority of the test data reported herein were measured during the P-3 power ascension. During the two-week period, the river water temperature remained essentially constant.

Some difference of opinion existed as to thermocouple location in P thermal shield. As a result of conversations with persons responsible for the installation of the thermocouples, and after study of the final as-built drawings (W-133178 and W-134168), it was concluded that thermocouples are padded on the shield inner wall at 3 positions (at 3/4 of the height from each shield tank bottom, at the midplane, and at 1/4 of the height from tank bottom). One thermocouple is padded at the midplane on the outer wall of each shield tank. There are also 9 thermocouples per tank which serve to follow changes in stream temperature.

In June 1954, the Technical Division was requested to determine the effectiveness of padded thermocouples in measuring metal surface temperature. There was a possibility that a loosely-peened pad would permit the shield coolant to lower the indicated surface temperature. The test results have not been published, but they show that peening had a negligible effect on the thermocouple reading.

Original Design Calculations

Prior to reactor startup at SRP, calculations were performed to confirm reactor soundness under thermal stress at maximum anticipated power levels. Most of the calculations were made to predict structural temperatures in the range 700 to 1400 MW. It was necessary, in some cases, to ratio design calculations down rather than extrapolate the data obtained. Calculated values from the following documents were either quoted or interpolated: DPEX-602, DPEX-451, DPWZ-1415, DPWZ-2510, DP-36, and DPE-772; (see references). In addition, data reported in DPSP 54-25-38 are analyzed.

Thermal Shield Stresses

This report does not concern itself with stress work; however, the temperatures presented should be useful in stress predictions. Of great concern in R and P reactors, from a stress standpoint, is the annular thermal shield. Two sketches of the shield follow.

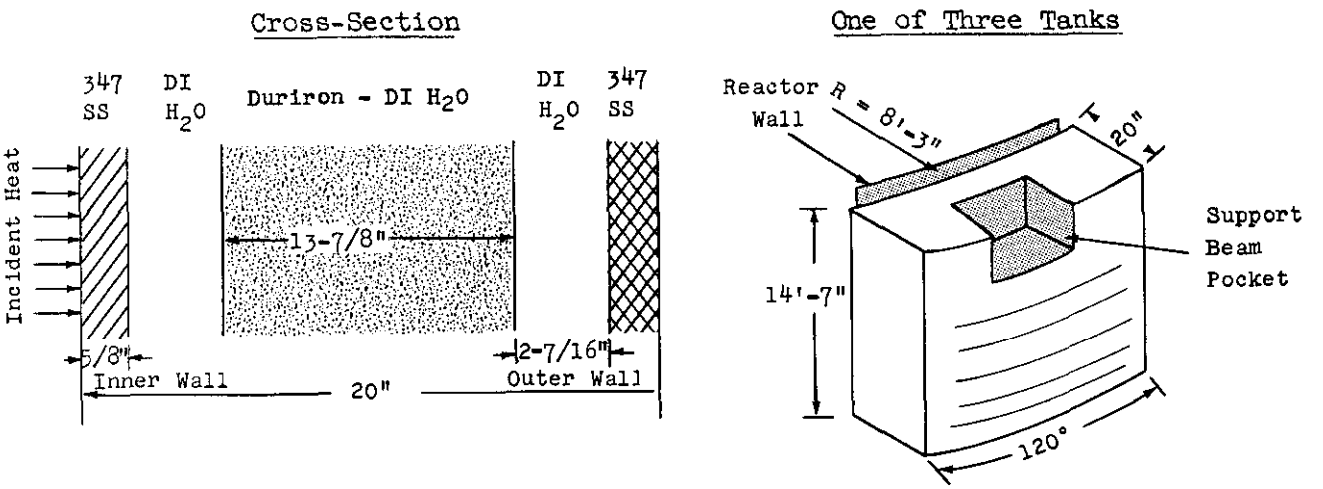

About one third of the heat flux incident on the inner wall of the thermal shield is attenuated in the 5/8-inch stainless steel inner wall. The heat generated is then transferred to the coolant flowing through the tanks. This heat load causes a temperature difference between the inner and outer walls. This temperature difference is a function of both total reactor power and longitudinal flux distribution.

The shield tanks may be considered as fixed on the bottom, and their circumferential expansion, when heated, produces negligible stresses. But the increased vertical motion of the inner wall over the outer wall sets up stresses in the corner of the support beam pockets and at the staybolts and instrument holes. These stresses may become critical at higher powers. A portion of this report presents reactor data for predicting shield stresses.

Test Measurement Equipment

Miscellaneous Temperature Monitor. This panel board consists of 10 rows or 40 telephone jacks used to measure structure temperatures. About 320 of the jacks are in use. One telephone plug may be used for instantaneous reading of any temperature on a Brown precision potentiometer, reading directly in degrees centigrade. A total of 64 plugs and 4 Brown precision temperature recorder potentiometers are provided for continuous tracking of any 64 temperatures. The use of the precision recorders in subsequent studies has been found to be more accurate for temperature data than use of the single point potentiometer.

Flow Metering Devices. Flow rate measurements of D_2O, deionized water, and river water flow to heat exchangers were made with standard flow metering orifices. The pressure drops across these orifices were transmitted by Brown 3 to 15-psi linear flow transmitters to the water graphic panel. Square root flow indicators were calibrated in gpm.

Pile Power Calculator. This instrument integrates and adds the product of flow times the difference in heat exchanger exit and inlet cooling water temperatures for each of 6 hydraulic systems feeding the reactor. For each system, the pressure drop across a metering orifice is converted to an AC signal proportional to the flow. This conversion is made by an inductance-coil transducer. The signal is then fed across 2 resistance-coil thermometers (thermohms), which measure H_2O exit and inlet temperatures, and whose difference in resistance is proportional to the temperature rise. Thus a voltage drop is produced across the resistance thermometers that is proportional to flow times temperature rise, or heat.

The output from each of the 6 systems is added on a static transformer and fed to an AC potentiometer which reads pile power directly in megawatts. The product of pile power and time is also integrated to give total fuel exposure time in megawatt-days.

Shield Temperature Recorder. A 12-point temperature recorder is provided for recording deionized water inlet and exit temperatures to the top, bottom, and annular thermal shields. River water inlet and exit temperatures to the shield heat exchangers are also recorded. The recorder is calibrated directly in degrees centigrade.

D_2O Temperatures. A jack box for measuring system inlet and exit thermohms is provided. The resistances were measured by a precision Rubicon bridge, and lead resistance was compensated for. System temperatures were then determined from calibration curves of the individual resistance thermometers provided by Technical Division.

Measurement Procedures

Telephone Plug Heating Correction. The majority of the data presented are temperatures measured on the Miscellaneous Temperature Jack Panel. Repeated use of the single telephone plug in hundreds of jacks introduces an error in the data, caused by heat-up of the plug from friction. The emf terminals in the plug are steel and brass, while the thermocouples and leads are iron-constantan. The dissimilar metal thermocouple formed at the plug adds an emf to the signal from the hot junction.

The error introduced by frictional heat-up of the plug varies from 2° to 4°C, depending on how tight the jack is and on how rapidly the plug is used. The error is not constant; ie, varying tightness of the jacks changes the error, even when the plug is inserted at a constant rate. In this study, the error was largely compensated for by periodically comparing the rise in isothermal box temperature over initial temperature, as indicated by one of the thermocouples in the isothermal box. It is known that the temperature in the isothermal box will not vary over the time required to take miscellaneous temperature data. Consequently, a reading of this box temperature after every 5th plug-in provides ample data to correct for heating the plug. This correction was made to the temperature data reported.

In a previous study done in the R-1 cycle, this correction for heating of the plug was not made (see DPSP 54-25-38). The reported data are high, and the error introduced is magnified when extrapolating R-1 temperature data to higher power levels.

The scheme used for correcting P-3 data is reasonable for extrapolating the data to higher powers, but is inferior to another method used successfully more recently. This involves using the miscellaneous temperature recorders. The recorders were re-ranged from 0-200°C to 0-100°C, the chart drive speed was increased to 4 inches/minute, and the recorders were calibrated to ± 0.2°C. This method eliminates all measurement errors, with the exception of the thermocouple error. Thus, for the most accurate reactor structure temperature data, use of the recorders is recommended.

Allowance for Equilibrium. Data indicate thermal equilibrium is reached in the shields after the initial rise from critical in about 2 hours, and in less than an hour for any subsequent power changes. All data reported were taken at least 2-1/2 hours after power change.

Data and Results

General Reactor Data. Figure 1, appendix, is a schematic cross section of R and P reactors. Representative reactor temperatures at each point on the sketch are presented for each power level in tables I through V, appendix. T_7, T_8, T_9, T_{10}, T_{11}, and T_{12} were

obtained from the shield temperature recorder, so that the absolute values cannot be compared with the temperatures obtained at the miscellaneous temperature jack panel, since one or both instruments could have been in error.

Figures 2, 18, and 19, appendix, show typical thermocouple installations in various reactor structures. The thermocouples in figures 18 and 19 are padded on the outer tank wall near its weldment to the bottom shield.

The longitudinal flux distribution in the reactor during the period data were collected is shown in figure 3, appendix. Flux measurements were made by oscillation of Gang III control rods (nearest the tank wall).

Thermal Shield. Reactor data on the thermal shield are given in table VI, appendix. The absolute values of inlet and exit temperatures can not be compared with wall and stream temperatures, since the two sets of data come from different instruments, both of which may be in error. It was decided to use the deionized water heat pickup in computing the percent of total reactor heat generated in the thermal shield, because heat is lost before the river water removes the heat in the heat exchanger.

Table VII, appendix, gives a breakdown of shield wall metal temperature differences (not to be confused with the surface temperatures which were measured), heat flux, and film coefficients. Two sets of data are presented, those calculated from reactor data, and those interpolated from design calculations.

Thermal Shield Calculations

Total Heat Generated

$$Q = MC\Delta T$$

where Q = heat generated, pcu/hr

M = lbs fluid flowing/hr

C = specific heat, pcu/lb-°C

ΔT = bulk temperature rise, °C

[redacted]

% Total Reactor Power Generated

$$\% = \frac{Q \times 100}{1.897 \times 10^6 \times \text{Pile Power}}$$

where Q = heat generated, pcu/hr

1MW = 1.897×10^6 pcu/hr

Pile Power = MW

Maximum Incident Heat Flux

$$E_{max} = \frac{Q}{\pi d A}$$

where E_{max} = maximum heat flux pcu/hr-ft^2

Q = heat generated, pcu/hr

d = shield inner diameter = 16.5 ft

A = area under figure 3, ft

Incident Flux On The Inner Wall At Height h

$$E_{O(h)} = Q_{N(h)} E_{max}$$

$E_{O(h)}$ = heat flux at point h

$Q_{N(h)}$ = normalized flux at point h, figure 3

E_{max} = maximum heat flux

[redacted]

[redacted]

Heat Flux Attenuated In Inner Wall at Point h

$$E_a = E_o - E_1$$

$$E_1 = E_o e - \mu x$$

$$E_a = E_o(1 - e^{-\mu x_1})$$

where x = wall thickness, ft

E_a = heat flux attenuated in x ft, pcu/hr-ft^2

E_o = incident flux, pcu/hr-ft^2

E_1 = transmitted flux, pcu/hr-ft^2

μ = attenuation coefficient, ft^{-1}

Film Coefficient From Inner Wall to Coolant

$$h = \frac{E_a}{t_s - t_f}$$

where h = film coefficient, pcu/hr-ft^2-°C

E_a = heat flux flowing through film from wall to coolant, pcu/hr-ft^2-°C

t_s = wall surface temperature, °C

t_f = fluid temperature, °C

[redacted]

Average Metal Temperature

$$h_o (t_o - t_{f_o}) = Bk + E_o$$

$$h_o \approx 0$$

Therefore

$$B = - \frac{E_o}{k}$$

$$t_o = t_1 - Bx - \frac{E_o}{\mu k} (1-e^{-\mu x_1})$$

$$t \text{ avg} = t_o + \frac{Bx_1}{2} + \frac{E_o}{\mu k} - \frac{E_o}{\mu^2 k x_1} (1-e^{-\mu x_1})$$

where

h_o = film coefficient on CO_2 side, pcu/hr-ft^2-°C

t_o = hot surface temperature, °C

t_{f_o} = hot side film temperature, °C

E_o = incident flux, pcu/hr-ft^2

x_1 = wall thickness, ft

t_1 = cold surface temperature, °C

t avg = average metal temperature, °C

B = a constant, °C/ft

μ = attenuation constant, ft^{-1}

k = conductivity, pcu/hr-ft^2-°C/ft

Design calculations were based on a flattop flux and on a greater heat load on the shield. Film coefficients were calculated from the DG standards. It is believed that the design predicted wall-to-wall temperature difference is higher because of a conservative estimate of heat generation in the thermal shield (about 0.63% of total reactor power).

Compensation was not made for the difference in the assumed shield coolant flow rate and the existing flow rate. Variations in flow rate will not have any significant effect on the comparison.

Figure 4, appendix, compares both maximum and length average wall-to-wall temperature differences as calculated by theory and from reactor data. Thermocouples do not exist on the upper and lower portions of the outer wall of the thermal shield. It was assumed that the outer wall temperature would be the same as the bulk coolant temperature at the same elevation. This assumption was also made in the theoretical approach, and it will be discussed in detail when the results are compared with design calculations.

Figure 5, appendix, reveals that design calculations are conservative in estimating the percent total reactor heat generated in the thermal shield. Reactor data have been collected from all SRP reactors (including the data in this report), and are presented as a band with a maximum and minimum. The plot is of great significance, since stress in the shield is a function of the heat generated.

Shield heat generation and heat removal data are presented in figures 6 and 7, appendix. The data were collected during the P-5 power ascension, using accurately calibrated instrumentation. The data are considered to be the most reliable of their kind collected to date.

Analysis of Other Temperatures. Figure 8, appendix, is a plot of average reactor D_2O inlet temperature and top shield deionized water inlet temperature variation with power. River water temperature has been subtracted from both curves, so the plot should be useful in predicting the relative motion of the D_2O plenum chamber and the shield at any time of the year, if the wrapper plate is assumed to be at the same temperature as the deionizer water in the shield (neglecting radiation effects).

A plot of reactor tank wall temperatures is presented in figure 9, appendix. If a graph of temperature versus elevation is made from the data, the temperatures will follow the flux distribution curve.

The reactor tank wall is welded to the bottom shield. A bending stress is produced at this T, and is a function of the upward deflection of the top plate of the bottom shield and the outward expansion of the tank, relative to the bottom plate of the bottom shield. The moment is clockwise. Temperature data useful for computing this stress are given in figure 10, appendix. Data collected in the R-1 cycle are also plotted. The R-1 data have no correction for telephone plug heat-up, so that they are not only initially displaced upward, but also spread as the error is multiplied by extrapolation.

Figure 11, appendix, presents the radial variation in surface temperature of the top and bottom plates of the bottom shield. Top plate thermocouples are padded on the deionized water side.

The variation of the difference between linear average top plate temperature and the bottom plate temperature of the bottom shield is plotted against reactor power in figure 12, appendix. Error in thermocouple readings displaces the curve below zero difference at 125 MW.

Figure 13, appendix, is useful in estimating the top plate temperature of the bottom shield at any time of the year. Note that the curve is for average temperature and not maximum. The curve would be displaced upward by a factor of about 1.5 for maximum top plate temperature.

Variation in top shield surface temperatures with power is given in figure 14, appendix. The average temperature of the top plate was assumed to be the average temperature of the deionized water in the shield.

Figure 15, appendix, presents temperature data for computing stress in the expansion joint. The curve gives the difference in outer and inner edge temperatures of the horizontal plate. In this discussion, the outer edge of the plate is defined as the edge nearer the reactor center.

Figure 16, appendix, is a plot of bearing ring temperature versus power. Based on reactor data, the temperature should increase about 3°C/100 MW.

The concrete shield structure surrounding the reactor apparently is not heated appreciably. Figure 17, appendix, compares concrete temperature at a point 3 inches from the 1/4-inch liner on the inner side of the concrete and at a point 3 feet away. Ambient temperature is also plotted, and the 2 concrete temperatures vary about ambient temperature and not power.

Figures 18 and 19, appendix, show typical thermocouples padded to the outer tank wall. These and all similar thermocouples indicate surface temperature.

Analysis of Results. The data collected in each step of the P-3 power ascension were corrected for heat-up of the telephone plug. The method of correction was not completely accurate, but it provided more meaningful results. It also makes extrapolation of the curves reasonable for predicting measured temperatures at higher powers.

For most of the results, an extrapolation was made merely by drawing the best straight line through the points. Other variables remaining constant, the temperatures should be linear with reactor power.

Comparison of Data with Design Calculations. In all cases where calculations were available, reactor structure temperatures have been compared with design calculations. In no case were design calculations below measured values.

The following assumptions were made in the design calculations.

- Thermal Shield (DPEX-602). The authors assumed natural circulation as the controlling flow mechanism, thus the flow through individual vertical channels is proportional to the heat transferred. If this is true, the temperature profile in any horizontal plane is constant, once the film temperature drop at the inner wall has been effected.

  Design calculations are given as the difference between integrated average metal temperature of the inner wall and stream temperature to represent the total difference between inner and outer wall temperatures. This was also assumed true for the upper and lower portions of the shield when reporting measured values.

- Heat Generation in the Thermal Shield (DP-36). The author based his calculations on an infinite slab pile. For a cylindrical pile with a cosine neutron flux in the buckled zone, the heat generated in the various portions of the thermal shield should be decreased by a constantly increasing factor as one moves from the center of the reactor.

- Top Shield (DPWZ-1415). Calculations were based on a tritium producing pile, which means a higher heat flux than if they were based on a plutonium producer.

- Bottom Shield and Tank Wall (DPWZ-2510). The author assumed the cold D_2O leaving blanket tubes (now Zone III fuel tubes) struck the tank wall before mixing with D_2O from fuel tubes.

- Bearing Ring and Expansion Joint (DPWZ-1415 and DPWZ-2510). Temperatures were computed assuming that the radiation guards (chimes) are 100% effective in shielding the bearing ring.

Appendix

[redacted]

TABLES

[redacted]

Table I. Miscellaneous Temperature Data at 50 MW

Location*	Temperature, °C	Temperature, °C		
		Tank A**	Tank B**	Tank C**
T_1		21.5	22.4	22.0
T_2		22.2	22.6	22.4
T_3		21.5	21.4	21.6
T_4		21.3	22.1	21.4
T_5		21.5	21.6	21.6
T_6		21.1	21.4	21.6
T_7	22.4			
T_8	23.0			
T_9	22.5			
T_{10}	22.5			
T_{11}	22.5			
T_{12}	22.7			
T_{13}	22.5			
T_{14}	22.7			
T_{15}	21.1			
T_{16}	22.6			
		At 30°† Location	At 240°† Location	
T_{17}		26.6	25.4	
T_{18}		27.4	26.6	
T_{19}		26.8	27.1	
T_{20}		25.2	26.5	
T_{21}		25.5	24.8	
T_{22}	23.5			
T_{23}	27.0			
T_{24}	26.9			
T_{25}	26.1			

* See figure 1.
** Tanks A, B, and C are thermal shield tanks.
† Thermocouple locations on the main tank wall are measured clockwise from X-2 (North).

Table II. Miscellaneous Temperature Data at 150 MW

Location	Temperature, °C	Temperature, °C		
		Tank A	Tank B	Tank C
T_1		23.9	27.0	25.2
T_2		23.6	24.8	23.9
T_3		23.5	22.8	23.4
T_4		22.7	23.5	23.0
T_5		22.7	23.5	22.8
T_6		22.5	22.5	23.0
T_7	23.9			
T_8	24.9			
T_9	23.6			
T_{10}	23.8			
T_{11}	23.8			
T_{12}	24.0			
T_{13}	23.7			
T_{14}	25.0			
T_{15}	24.5			
T_{16}	23.9			
		At 30° Location	At 240° Location	
T_{17}		30.8	29.9	
T_{18}		34.4	34.2	
T_{19}		36.1	36.1	
T_{20}		36.2	35.5	
T_{21}		31.2	30.4	
T_{22}	26.6			
T_{23}	25.6			
T_{24}	25.1			
T_{25}	26.0			

Table III. Miscellaneous Temperature Data at 300 MW

Location	Temperature, °C	Temperature, °C		
		Tank A	Tank B	Tank C
T_1		25.9	30.3	28.2
T_2		28.9	30.4	29.2
T_3		26.3	24.7	25.9
T_4		24.0	25.8	24.9
T_5		24.6	25.1	24.8
T_6		23.8	24.3	24.4
T_7	25.8			
T_8	27.2			
T_9	25.0			
T_{10}	25.5			
T_{11}	25.5			
T_{12}	26.0			
T_{13}	25.3			
T_{14}	28.9			
T_{15}	29.4			
T_{16}	25.8			
		At 30° Location	At 240° Location	
T_{17}		36.9	36.1	
T_{18}		43.3	42.5	
T_{19}		46.7	45.1	
T_{20}		46.7	47.4	
T_{21}		39.1	41.6	
T_{22}	31.0			
T_{23}	30.4			
T_{24}	29.1			
T_{25}	25.8			

[redacted]

Table IV. Miscellaneous Temperature Data at 370 MW

Location	Temperature, °C	Temperature, °C		
		Tank A	Tank B	Tank C
T_1		28.6	32.1	29.5
T_2		30.3	31.5	30.5
T_3		27.4	25.9	27.0
T_4		25.5	26.8	25.8
T_5		25.0	26.6	25.7
T_6		25.4	25.6	25.3
T_7	27.2			
T_8	28.8			
T_9	26.5			
T_{10}	27.1			
T_{11}	27.1			
T_{12}	27.1			
T_{13}	26.8			
T_{14}	31.4			
T_{15}	32.4			
T_{16}	27.4			
		At 30° Location	At 240° Location	
T_{17}		40.0	41.2	
T_{18}		50.1	52.4	
T_{19}		52.2	55.0	
T_{20}		50.2	52.5	
T_{21}		43.4	45.2	
T_{22}	32.9			
T_{23}	34.5			
T_{24}	32.8			
T_{25}	26.1			

[redacted]

Table V. Miscellaneous Temperature Data at 410 MW

Location	Temperature, °C	Temperature, °C		
		Tank A	Tank B	Tank C
T_1		29.3	33.2	30.3
T_2		31.1	32.7	31.3
T_3		28.2	26.2	27.8
T_4		26.4	27.0	26.2
T_5		26.1	26.4	26.1
T_6		26.0	25.9	26.0
T_7	28.4			
T_8	30.1			
T_9	27.7			
T_{10}	28.4			
T_{11}	28.4			
T_{12}	29.0			
T_{13}	27.8			
T_{14}	33.0			
T_{15}	35.0			
T_{16}	28.8			
		At 30° Location	At 240° Location	
T_{17}		41.5	41.9	
T_{18}		51.6	52.2	
T_{19}		54.9	54.0	
T_{20}		51.9	54.0	
T_{21}		43.2	44.1	
T_{22}	34.5			
T_{23}	35.6			
T_{24}	33.8			
T_{25}	28.4			

Table VI. Thermal Shield Data

	Reactor Power, MW					
	0	50	150	300	370	410
River Water Temp In, °C	23.5	22.3	22.4	22.6	23.3	24.3
River Water Temp Out, °C	23.2	22.6	24.0	25.6	26.9	28.3
Annular Shield DI Water Temp In, °C	23.2	22.4	23.9	25.8	27.2	28.4
Annular Shield DI Water Temp Out, °C	23.5	23.0	24.9	27.2	28.2	30.1
Shield Temp (avg of 3 tanks) at location:						
1*		22.0	25.4	28.1	30.1	30.9
2*		22.4	24.1	29.5	30.8	31.7
3*		21.5	23.2	25.6	26.8	27.4
4†		21.6	23.1	24.9	26.0	26.5
5**		21.6	23.0	24.8	25.8	26.2
6†		21.4	22.7	24.2	25.4	26.0
Total Heat to Annular Shield from						
DI Water flow × ΔT, Pcu/hr × 10^{-6}	0.245	0.489	0.815	1.141	1.304	1.386
River Water flow × ΔT, Pcu/hr × 10^{-6}	-0.086	+0.086	0.456	0.855	1.026	1.140
% Total Reactor Power based on DI water Heat pickup		0.515	0.286	0.248	0.186	0.178
Shield Water Flow Rate‡, gpm = 1630						
River Water Flow Rate‡, gpm = 570						

* Padded on inner wall.
** Padded on outer wall.
† Stream temperature.
‡ Shield and river water flow rates were measured by flow metering orifices.

Table VII. Comparison of Reactor Data and Design Calculations on the Annular Thermal Shield

Reactor Data (avg of 3 tanks)	Reactor Power, MW					
	0	50	150	300	370	410
Max Heat Flux, Pcu/hr-ft² (based on deionized water heat pickup, area under figure 3, and the shield ID = 16.5')	483	965	1608	2251	2573	2735
Avg Heat Flux, Pcu/hr-ft² (based on figure 3; q_{max}/q_{avg} = 1.53)	315	629	1048	1468	1678	1783
Max (midplane) Film ΔT, °C	not taken	0.8	1.1	4.7	5.0	5.5
Heat Flux, E_a, Passing Through Film at Midplane, Pcu/hr-ft²	147	293	489	684	782	831
Inner Wall Film Coefficient, Pcu/hr-ft²-°C (h - E_a/ΔT film)	-	366	444	146	156	151
Shield Wall to Wall ΔT, Difference in Integrated Avg Metal Temperature, °C, at positions: cosine						
1	not taken	1.0	3.2	4.5	5.5	5.9
2		1.3	2.1	6.1	6.6	7.2
3		0.8	1.3	2.6	2.5	2.7
4 linear average		1.0	2.2	4.4	4.9	5.3
Design Calculations (DFEX-602)						
Total Heat Load on Shield, Pcu/hr × 0^{-6}	0	0.591	1.785	3.570	4.403	4.879
Maximum Heat Flux, Pcu/hr-ft²	0	877	2631	5262	6490	7191
Avg Heat Flux, Pcu/hr-ft² (based on q_{max}/q_{avg} = 1.62)		541	1623	3247	4004	4437
Midplane Heat Flux Through Film, Pcu/hr-ft²		194	580	161	432	1587
Film Coefficient, Pcu/hr-ft² °C (DG 7.02C)		85	87	108	113	118
Integrated Avg Metal Temperature difference Between Inner and Outer Wall, °C, at positions: Flattop						
1		0.7	2.3	4.7	5.9	6.6
2		0.9	2.9	5.7	7.0	7.7
3		1.1	3.2	6.5	8.1	9.0
4 linear average		0.9	2.6	5.2	6.4	7.1

FIGURES

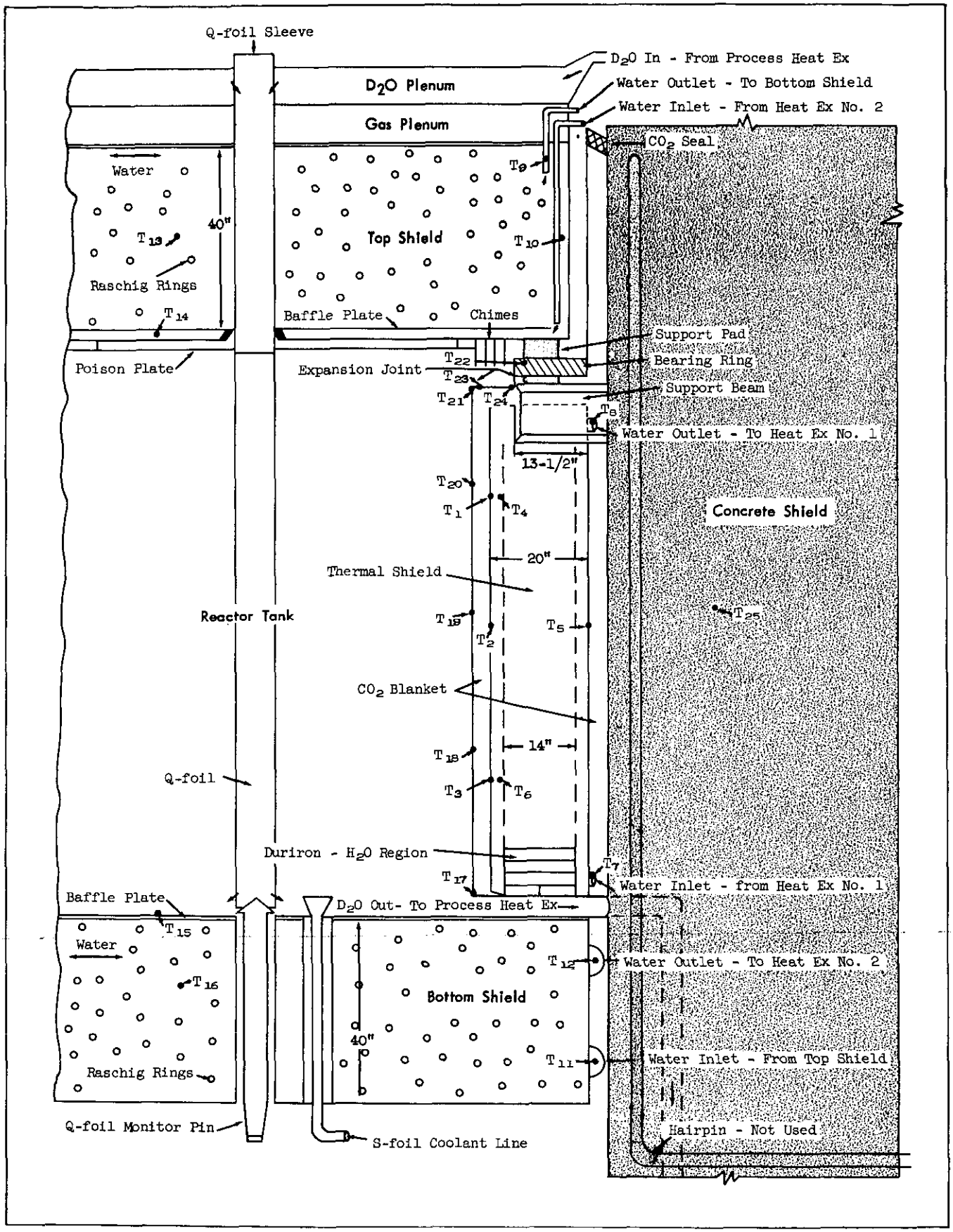

Figure 1. R and P Center Section Structures

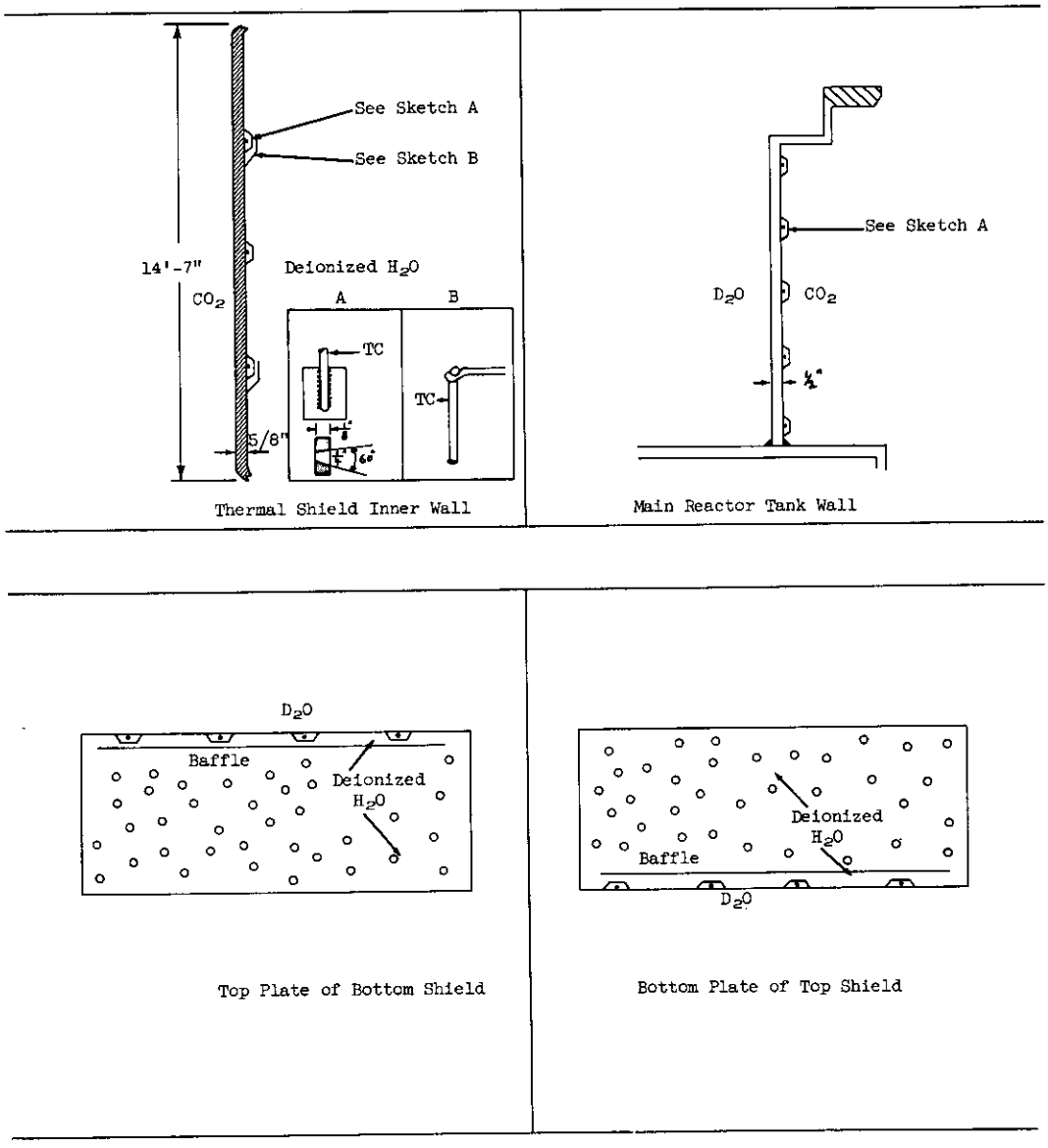

Figure 2. Schematic Diagram of Thermocouple Locations

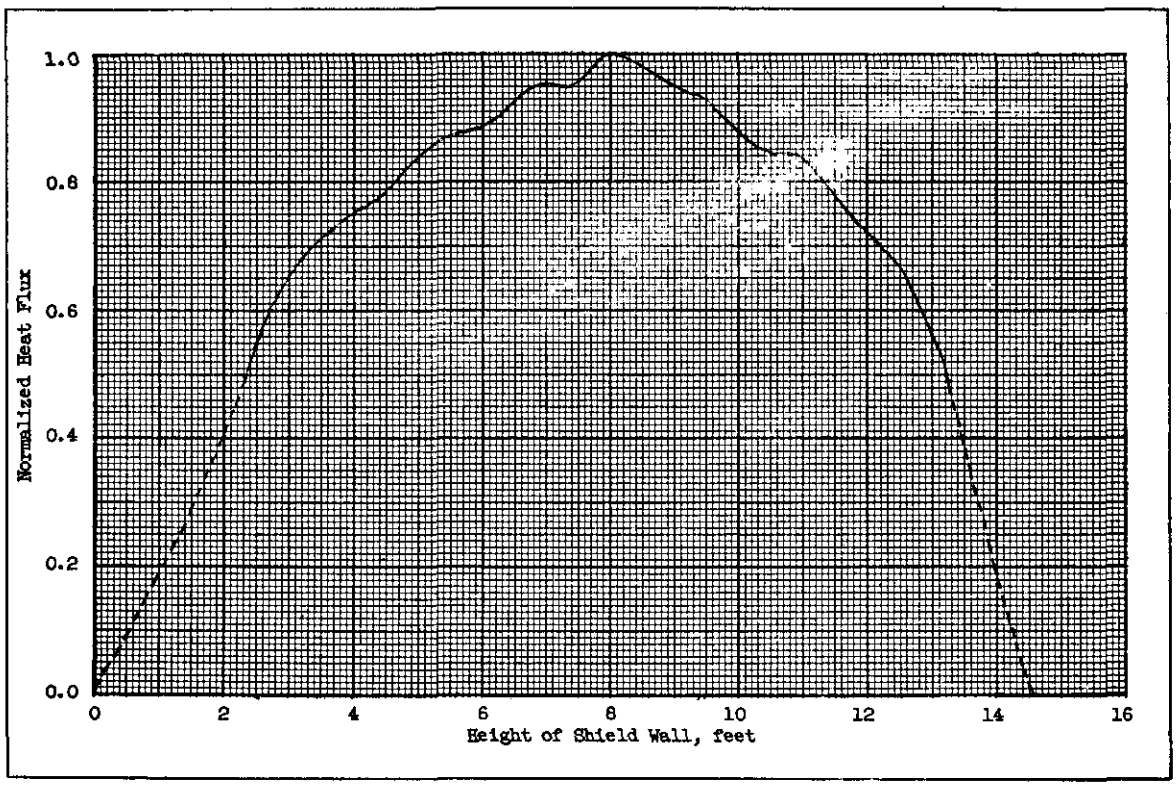

Figure 3. Longitudinal Flux Measured in P Reactor by Rod Oscillation On 10/15/54 - Gang III.

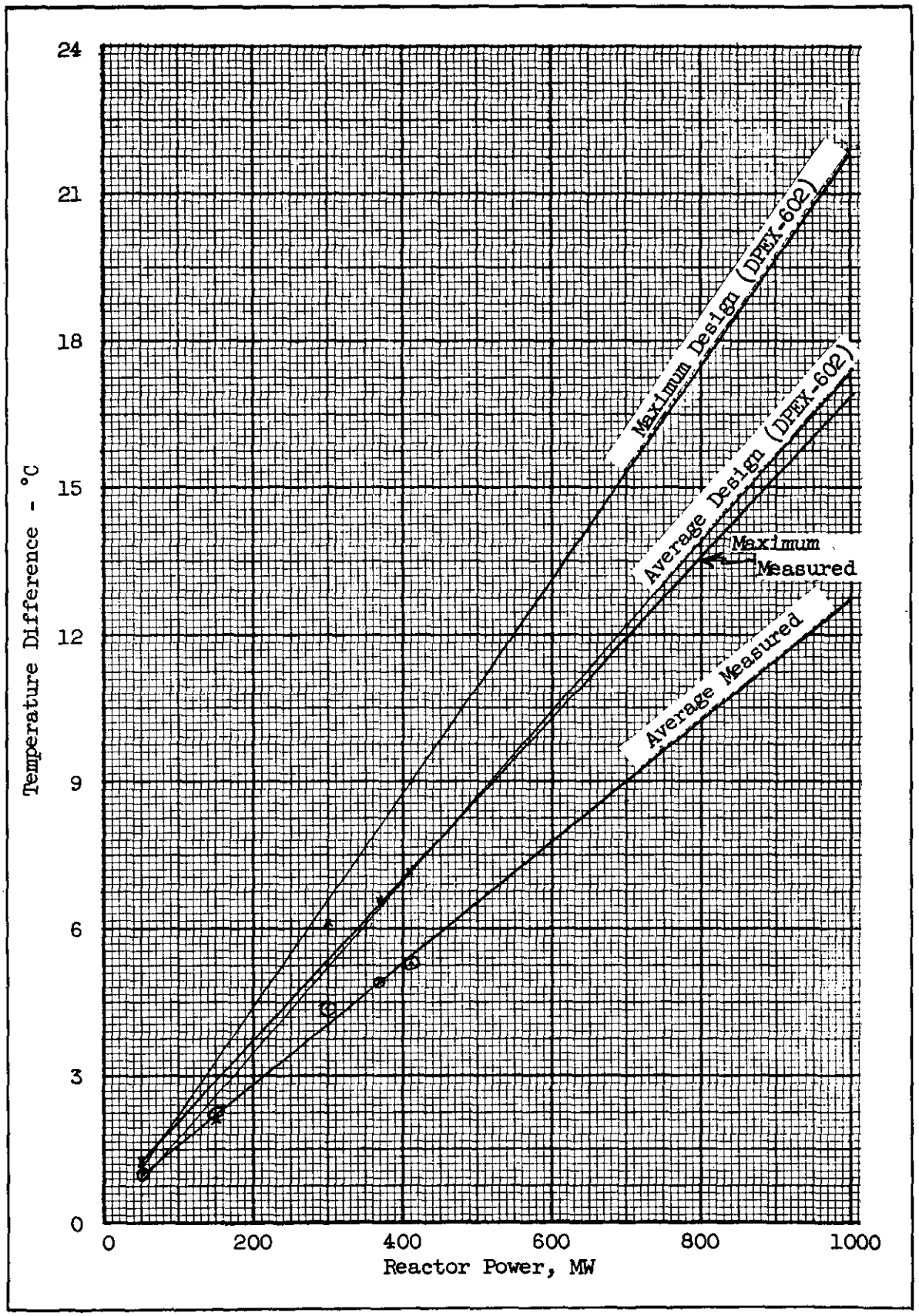

Figure 4. Thermal Shield - Metal Temperature Difference Between Inner and Outer Walls.

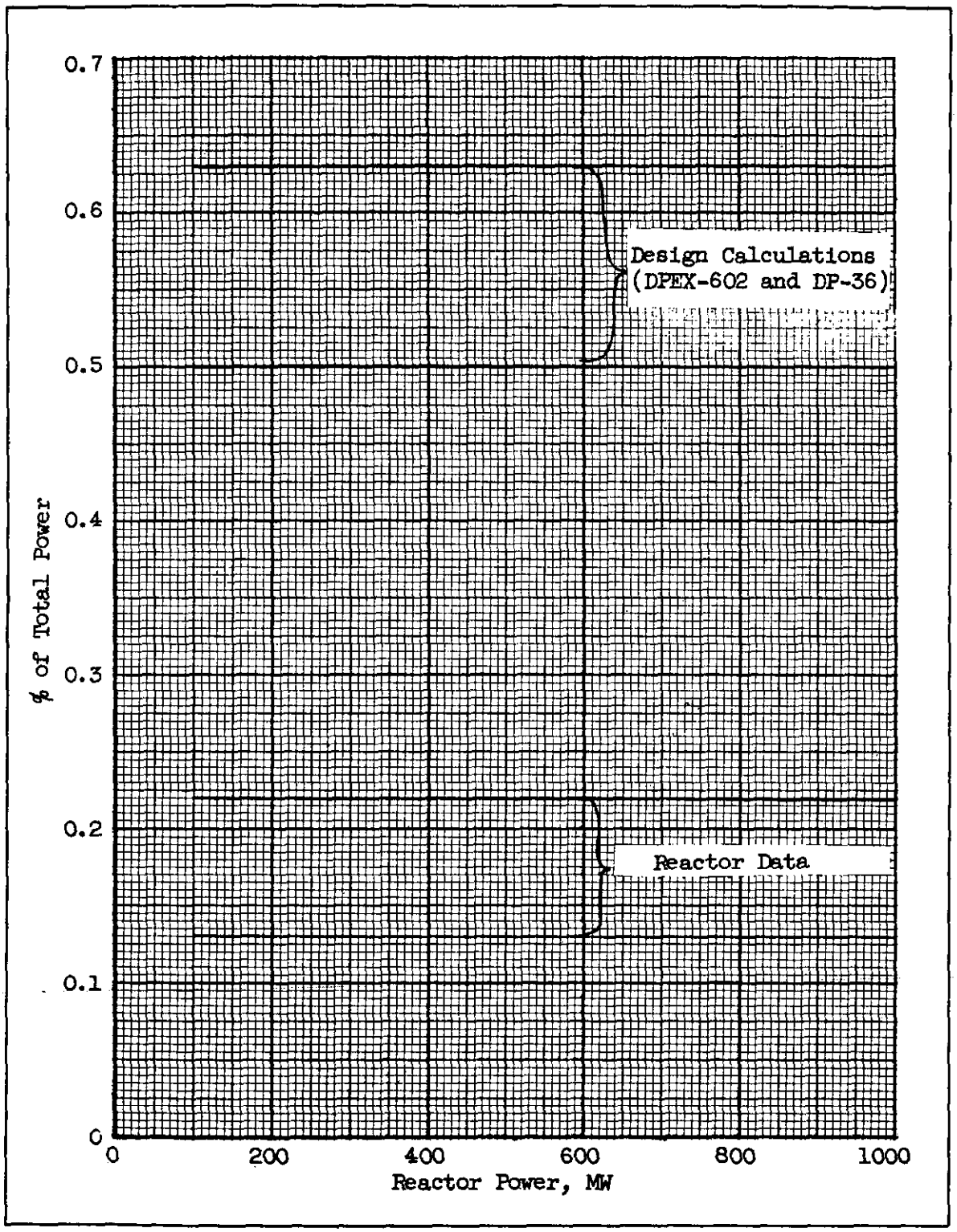

Figure 5. Heat Generated In The Thermal Shield

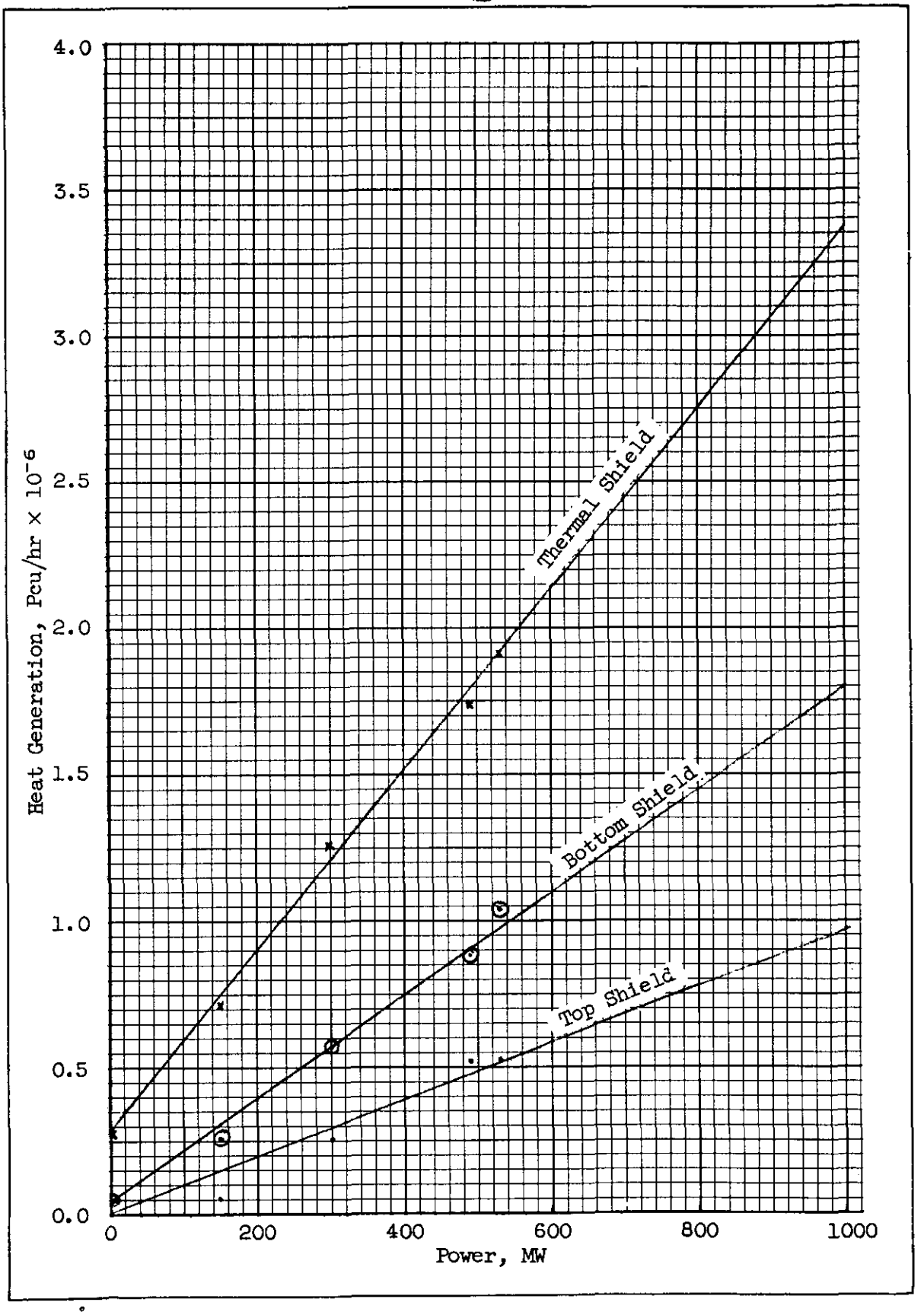

Figure 6. Heat Generated In The Shields.
P-5 Study

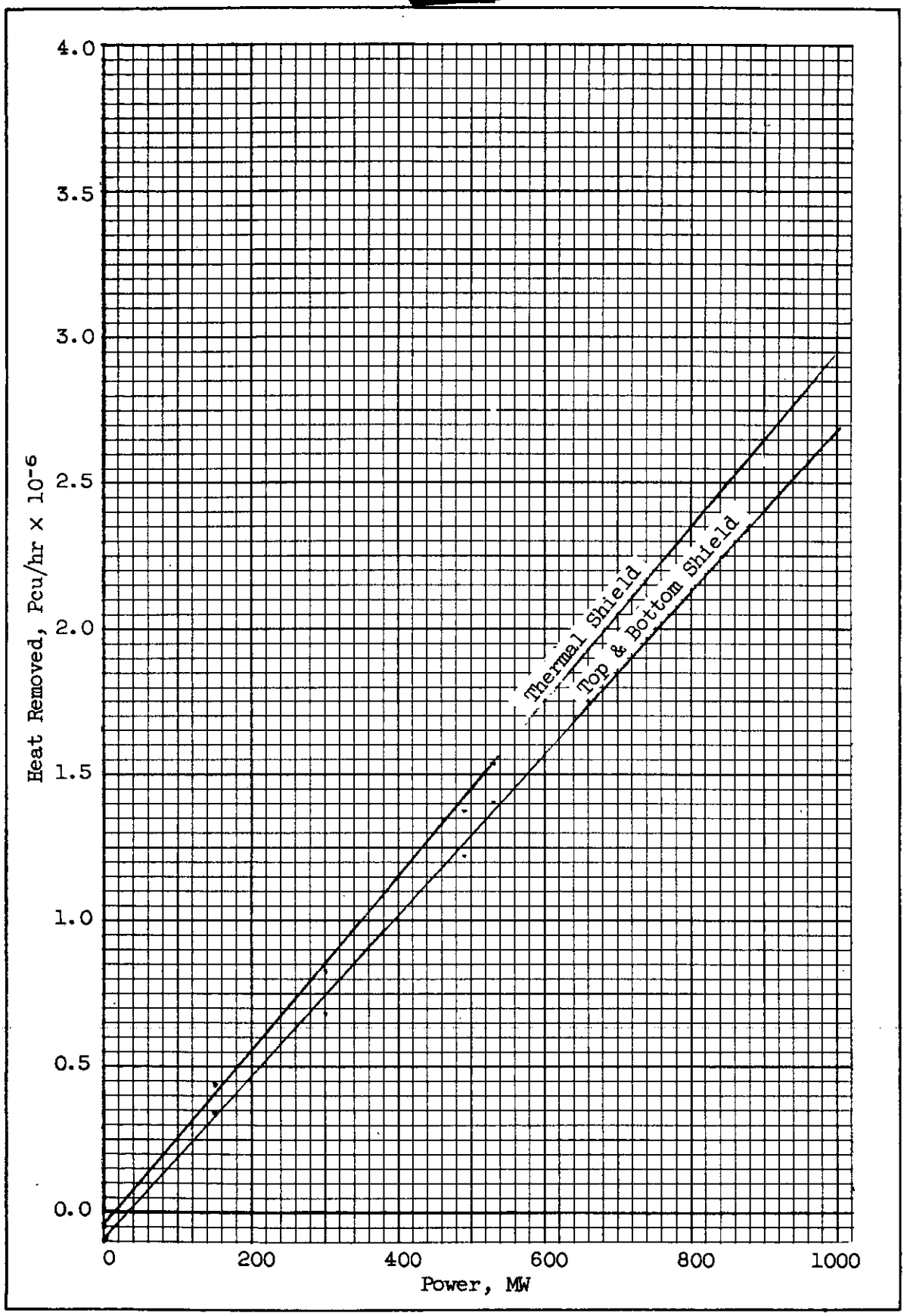

Figure 7. Heat Removed In The Shield Heat Exchangers.
P-5 Study

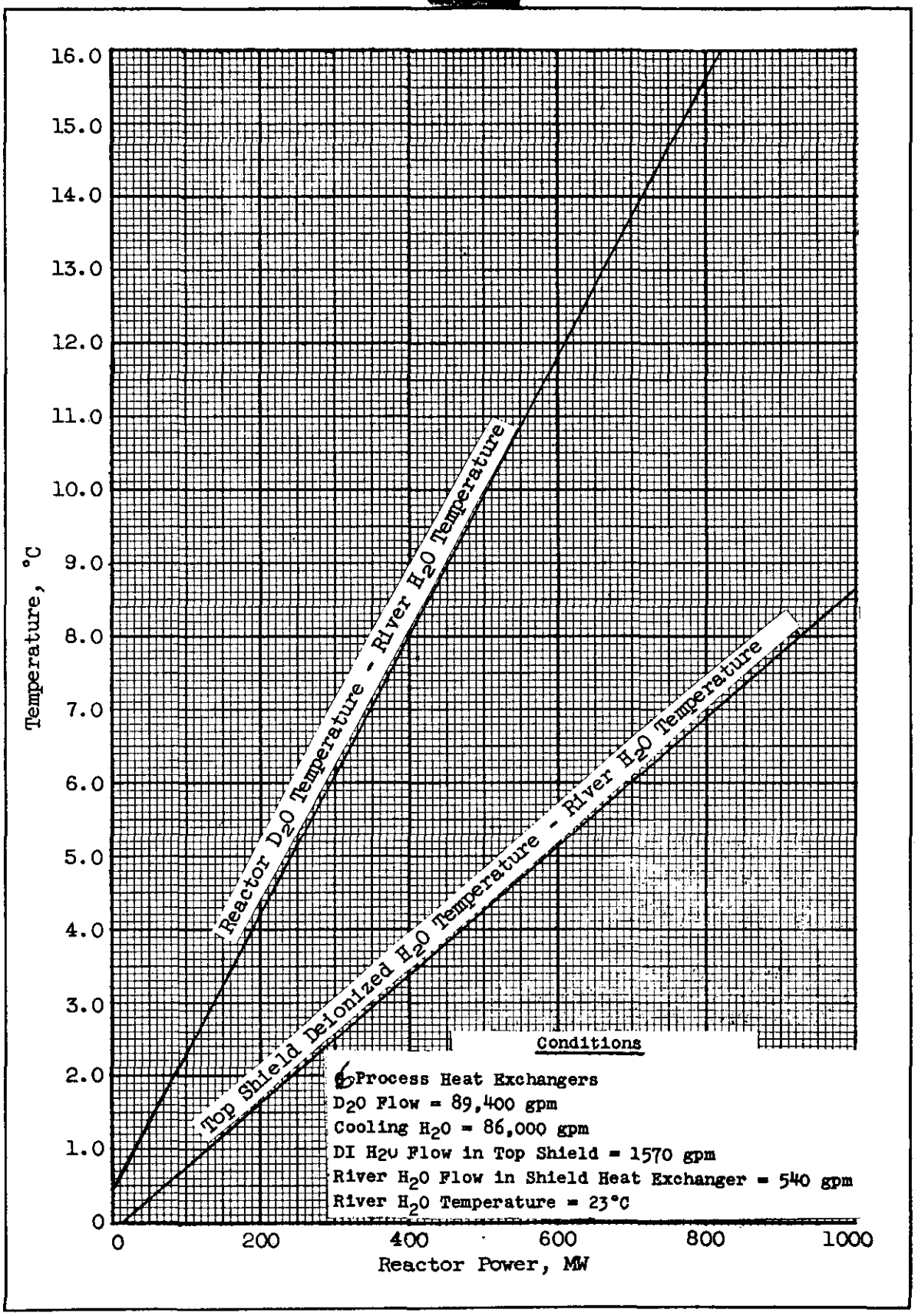

Figure 8. Relative Inlet Temperatures of D_2O And DI H_2O To Top Shield

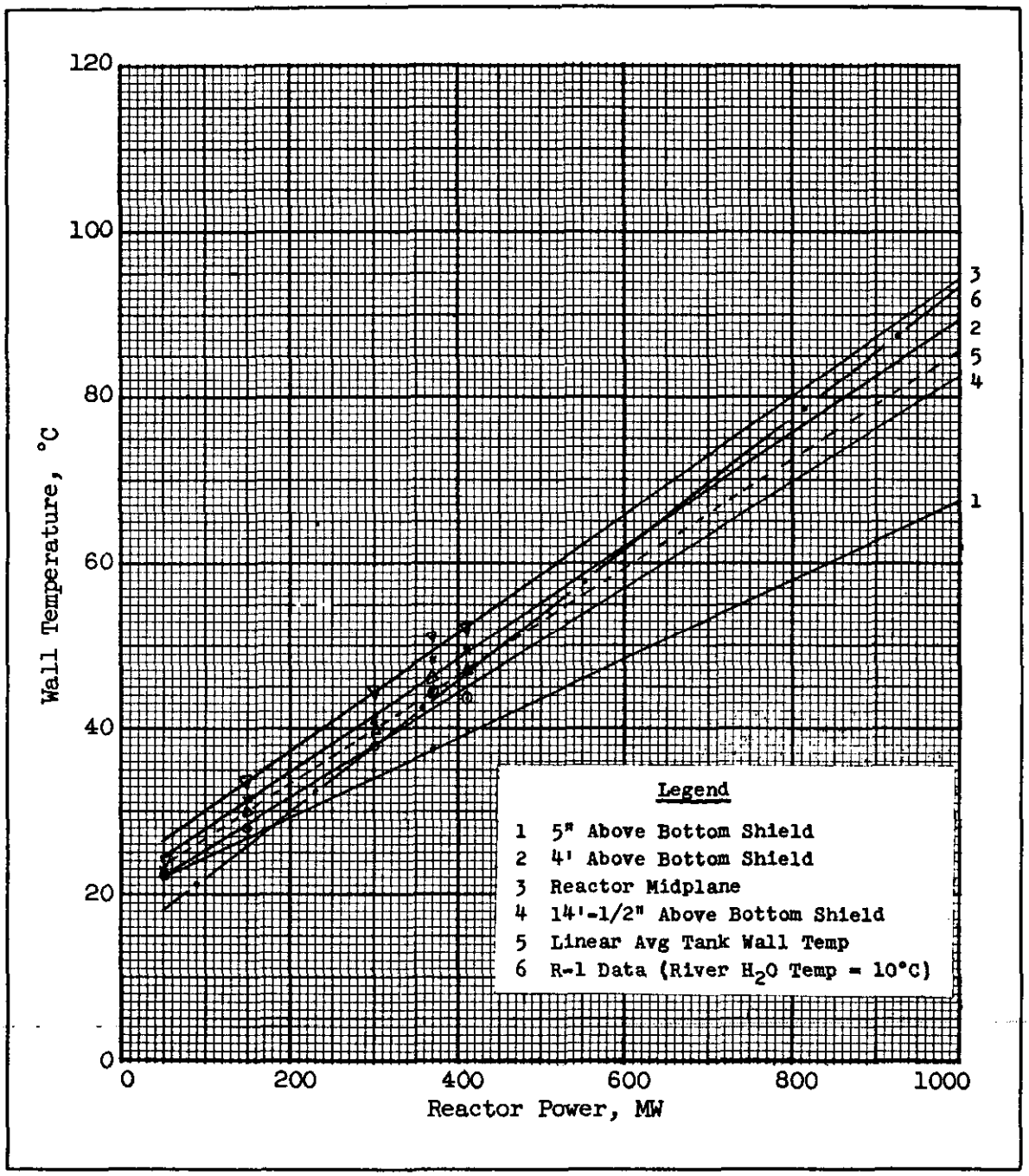

Figure 9. Reactor Tank - Outer Wall (CO_2 Side) Surface Temperatures (River Water Temp = 23°C)

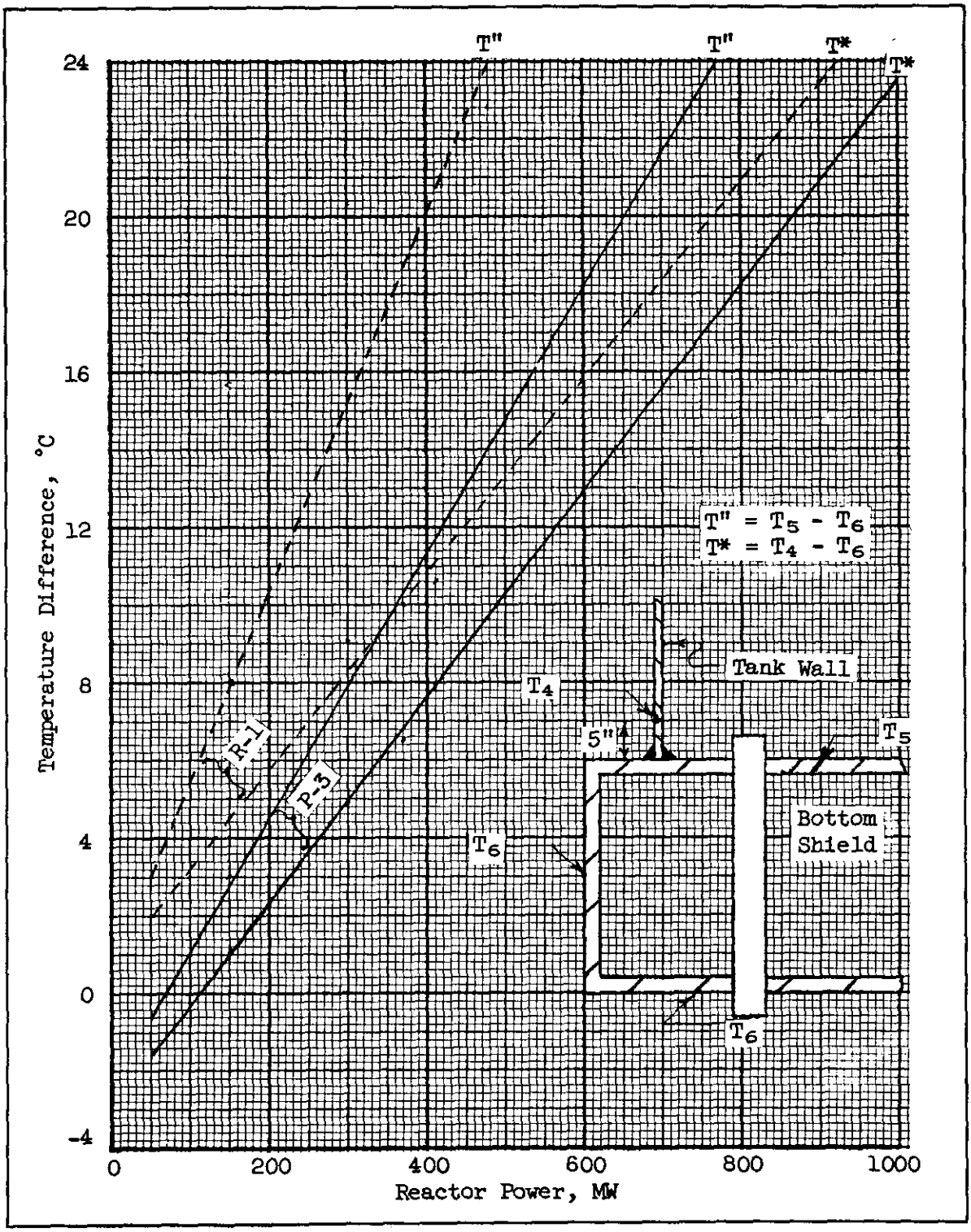

Figure 10. T-Weld Temperature Differences
Note: The curves present surface temperature differences - not differences in metal temperature.

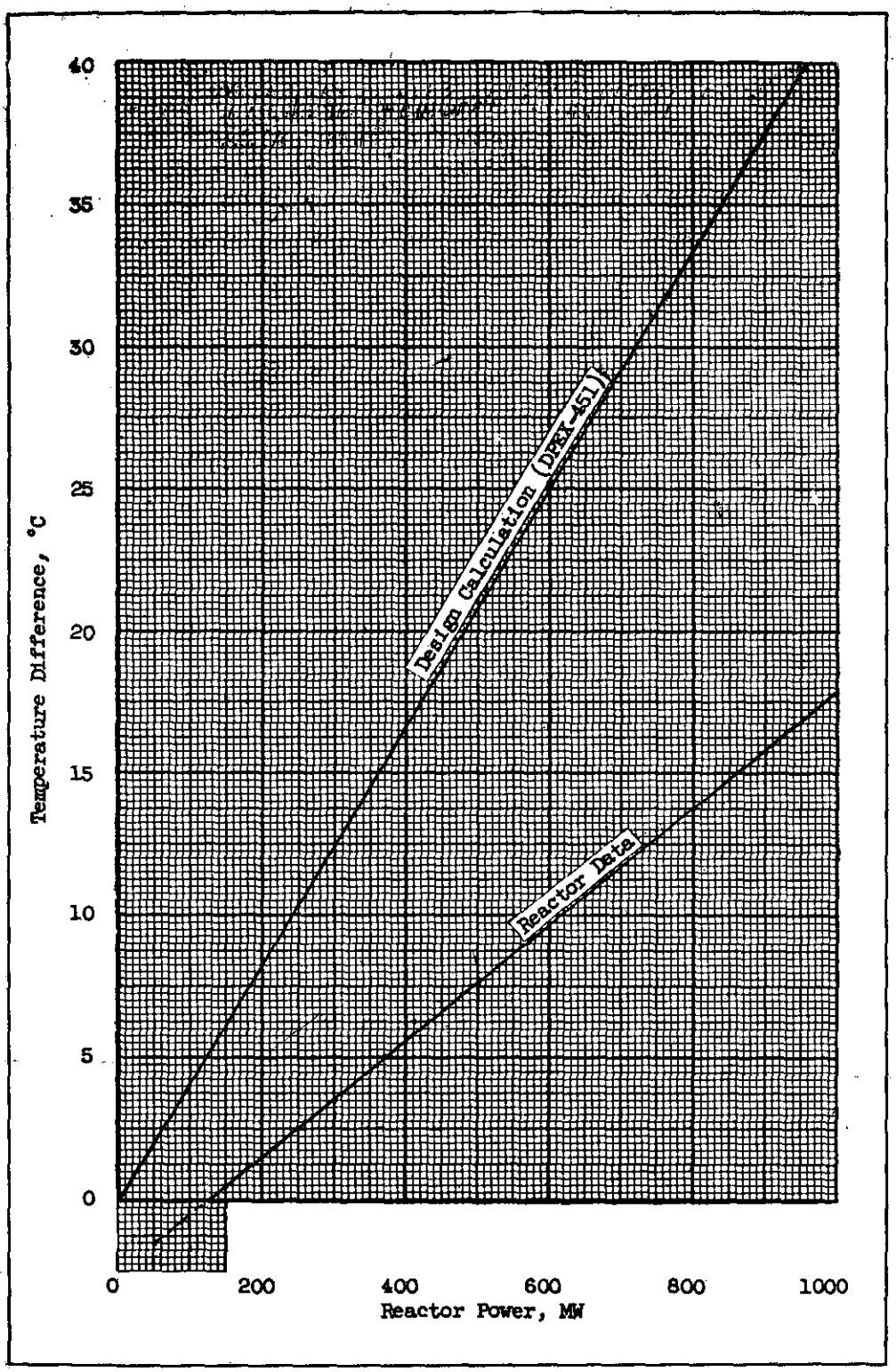

Figure 11. Radial Temperature Distribution - Bottom Shield

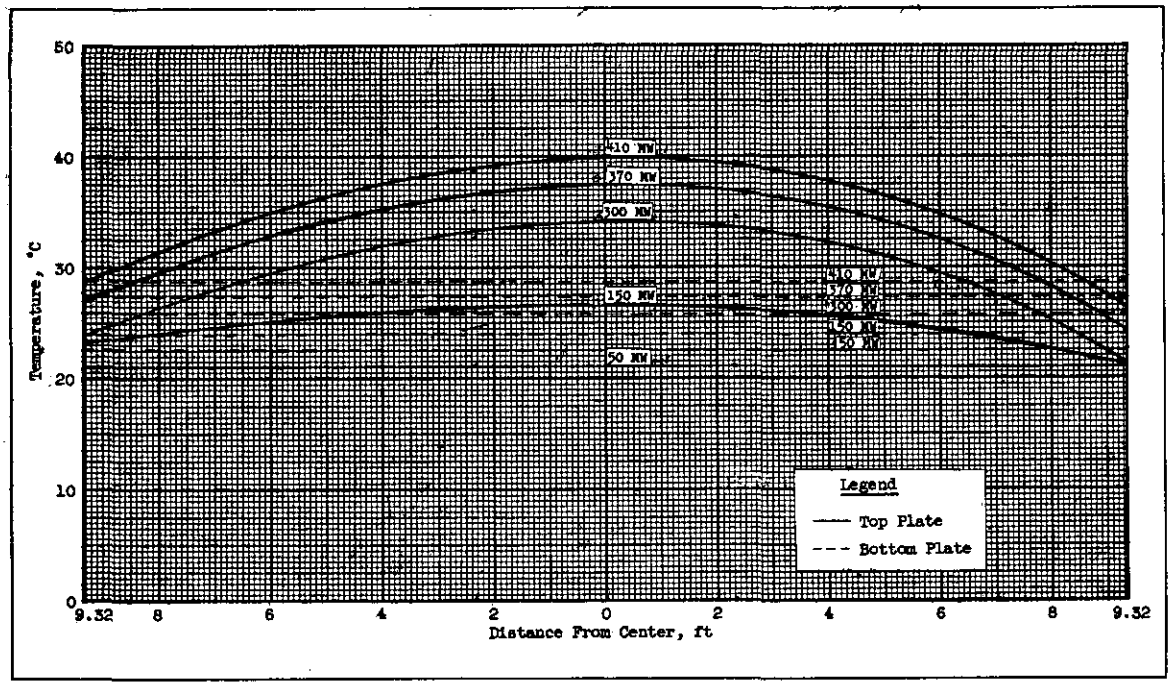

Figure 12. Bottom Shield
Linear Average Top Plate Temperature
Minus Temperature of Bottom Plate
Note: The curves present differences in surface temperatures and not metal temperatures.

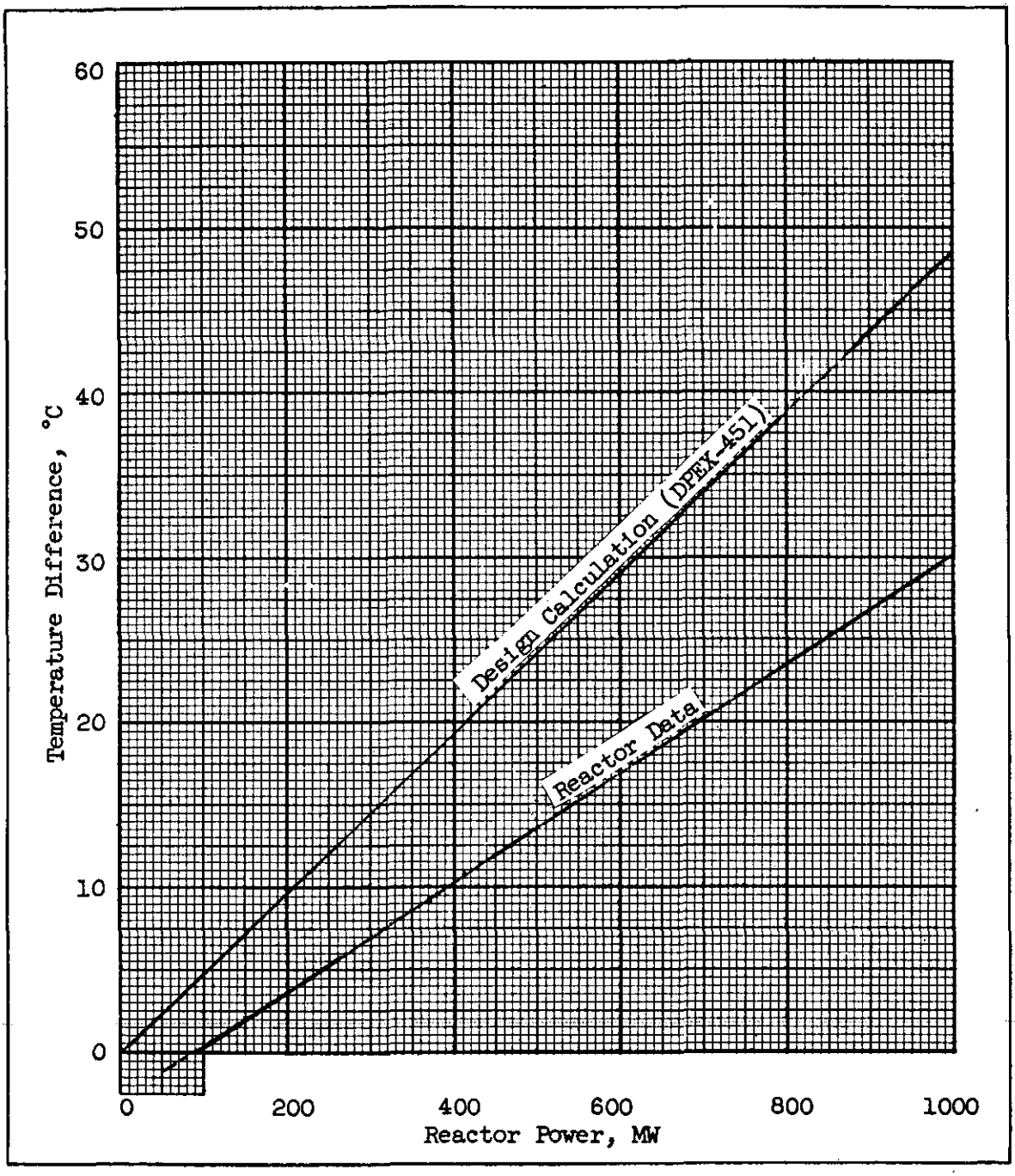

Figure 13. Bottom Shield
Linear Average Surface Temperature of
Top Plate Minus River Water Temperature

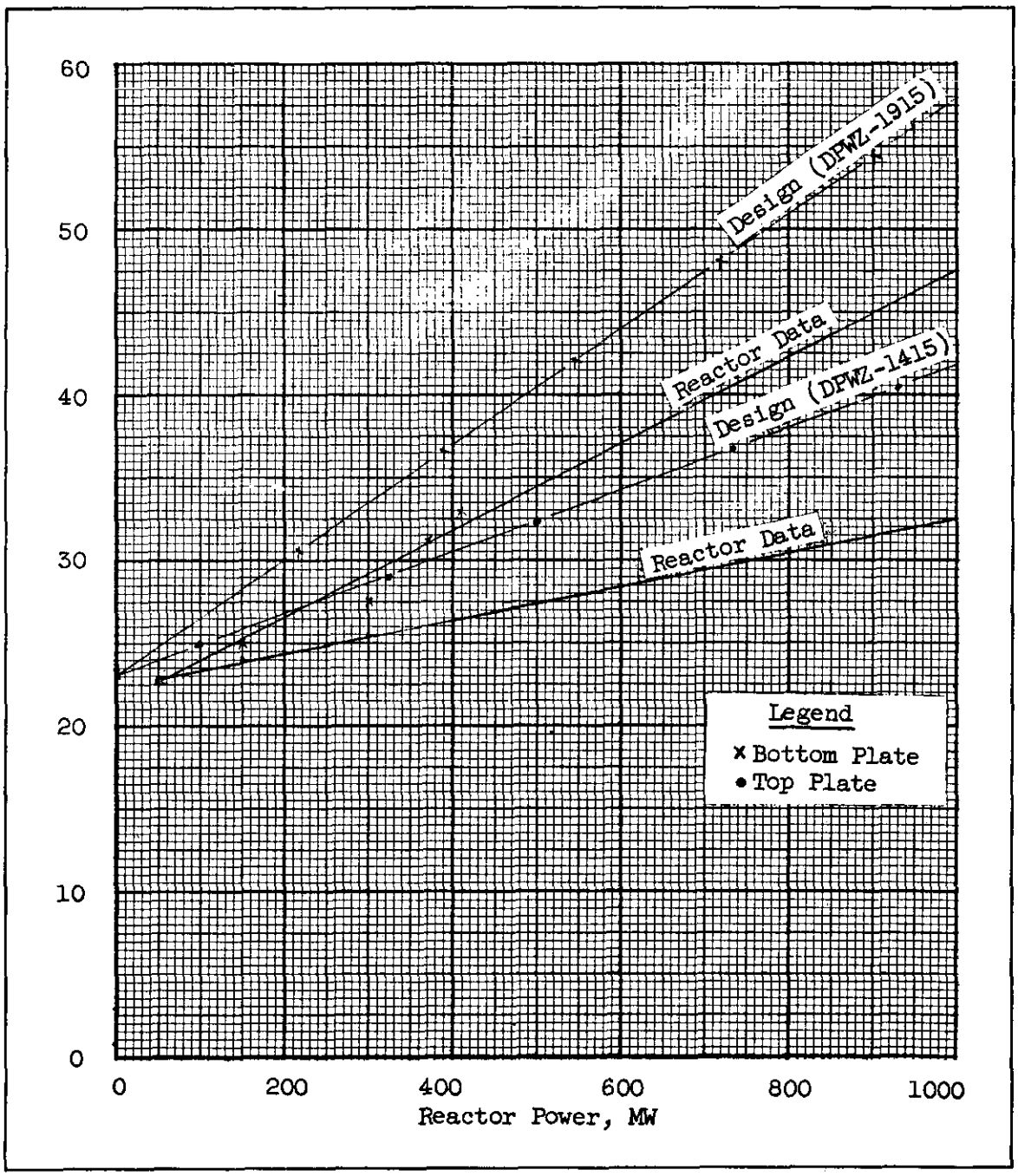

Figure 14. Top Shield
Top and Bottom Plate Temperatures

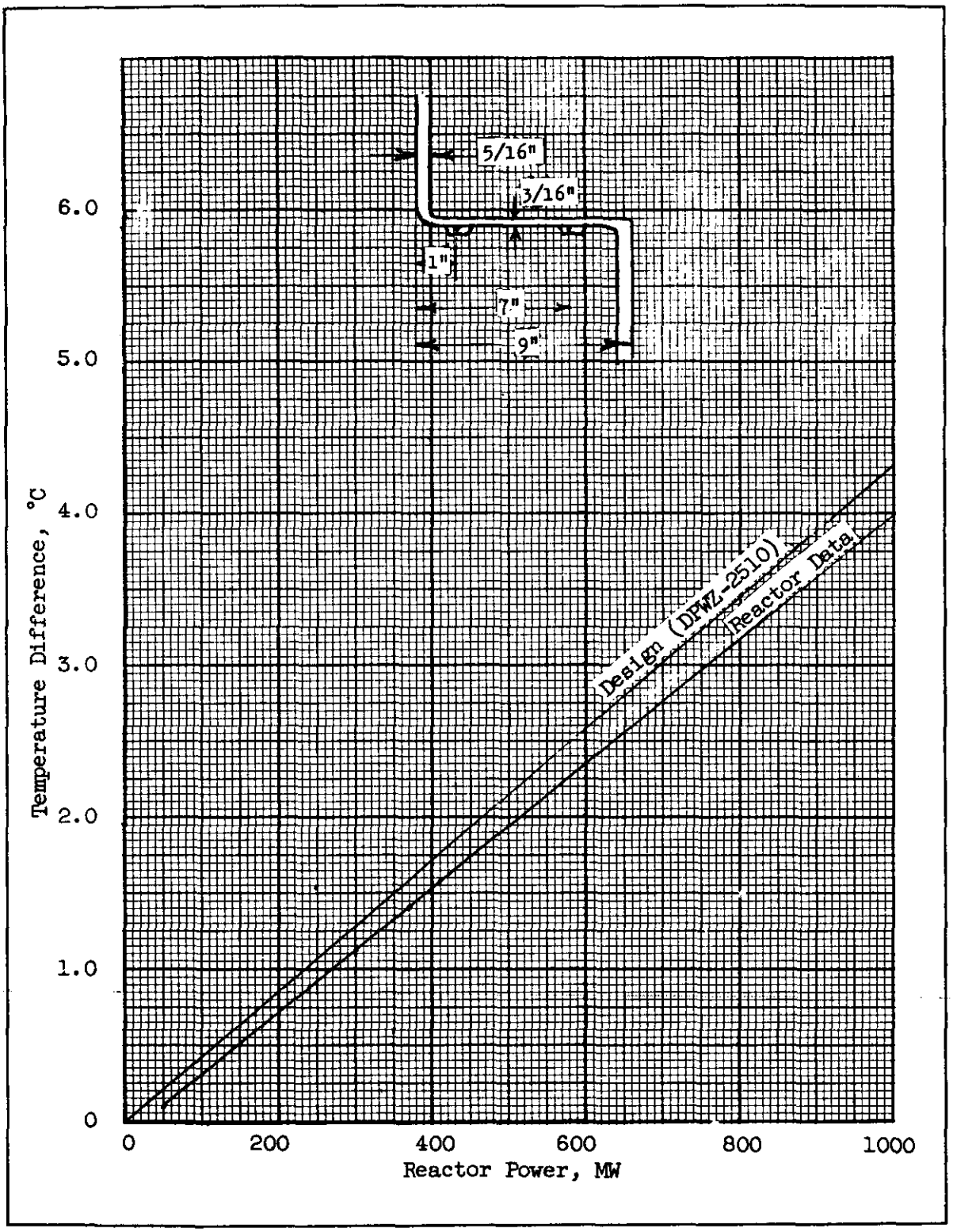

Figure 15. Expansion Joint Temperature Difference - Temperature at Outer Edge Minus Temperature at Inner Edge

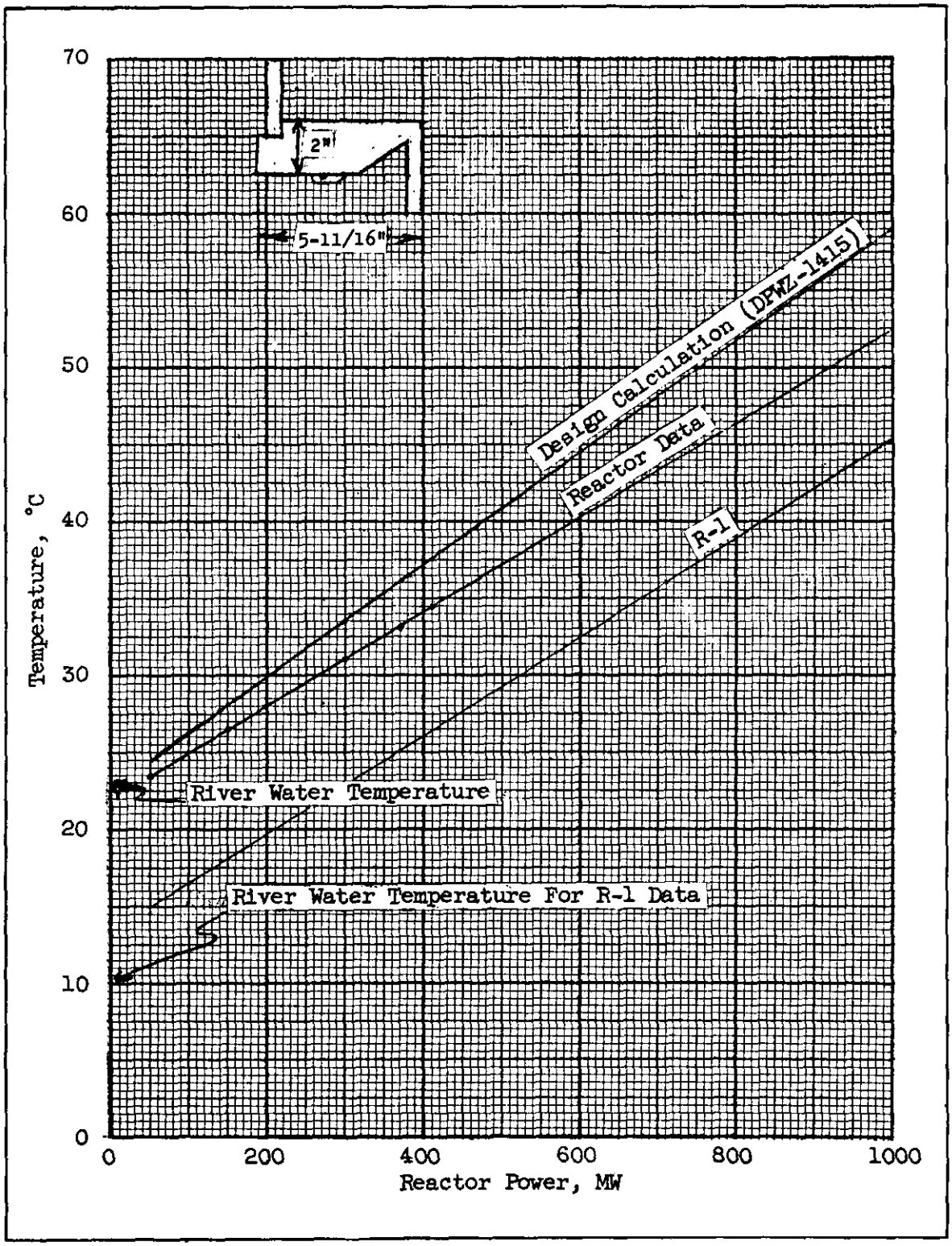

Figure 16. Bearing Ring Temperature

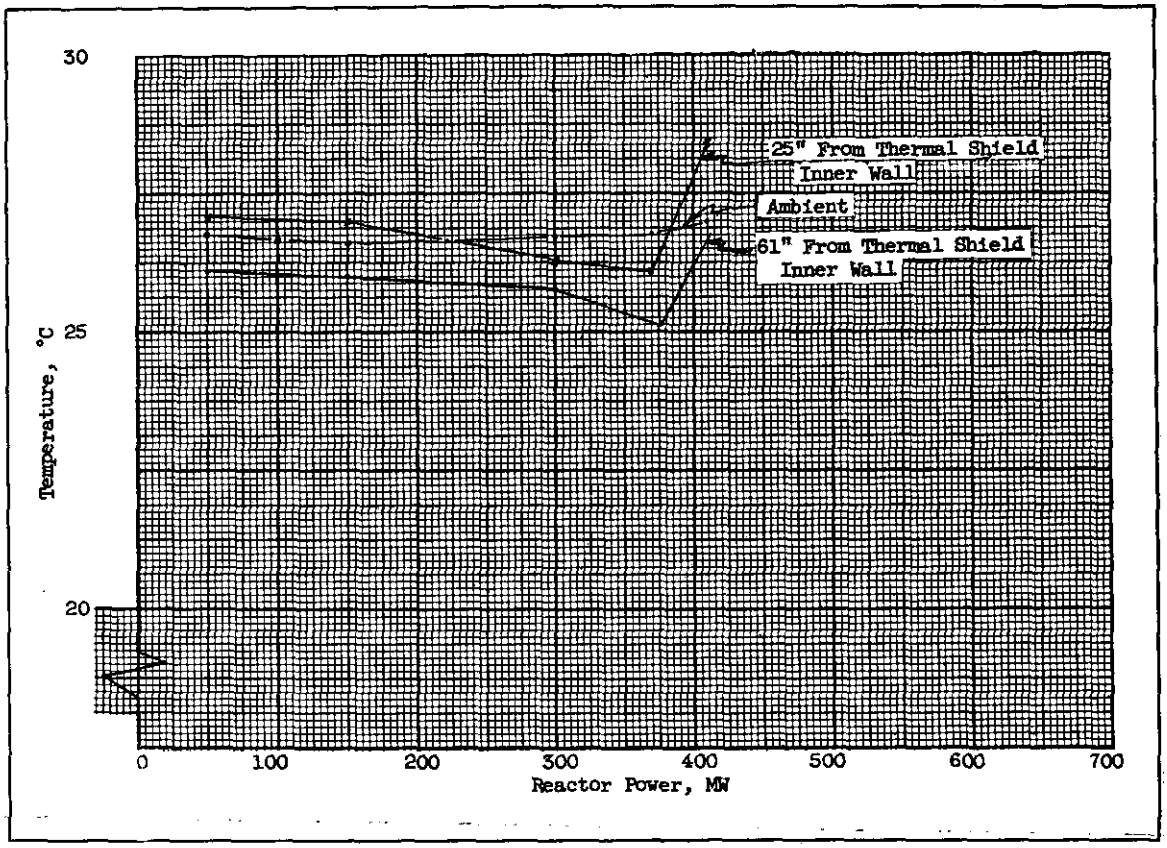

Figure 17. Concrete Temperature

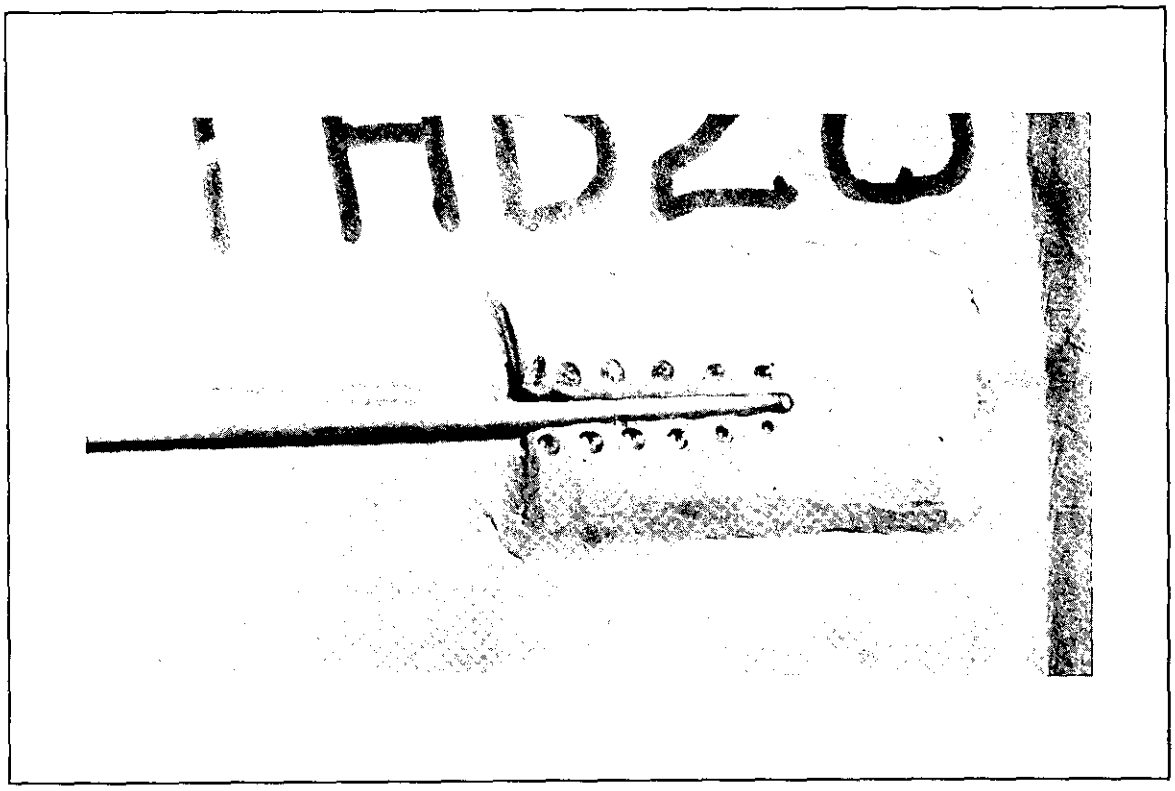

Figure 18. Thermocouples on Tank Wall - Near Bottom Shield

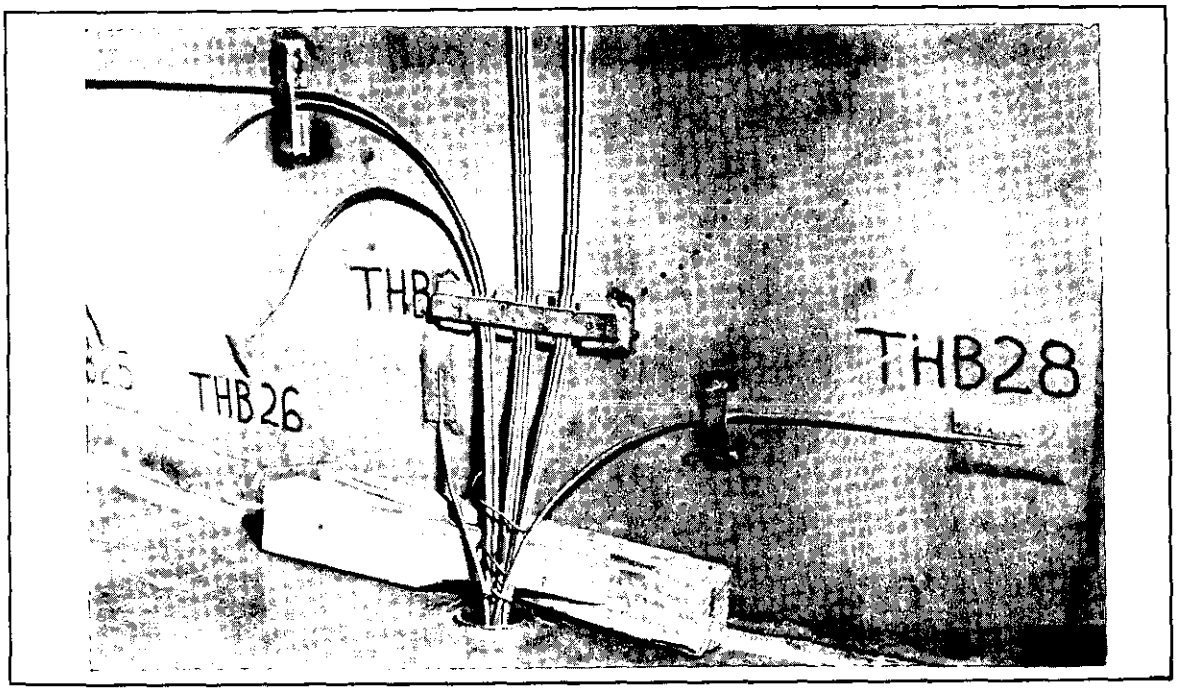

Figure 19. Typical Thermocouple Padded On Wall

References

Barker, D. H. and Cichelli, M. T., "Temperature Distribution in the Walls of the Annular Thermal Shield", DPEX-602.

Brinn, M. S. "Reactor Metal Temperatures for 1400 MW Operation", DPWZ-2657; "Thermal Stresses in Tank Structure", DPEX-451; "Expansion Joint and Bearing Ring Temperatures at 700 MW Power Operation", DPWZ-2510; and "Thermal Stresses in Structural Members of Pile", DPWZ-1415.

Brown, R. B. and Hoefer, J. A., "R Reactor Motion and Stress Analysis", DPSP 54-25-38.

Clark, H. K., "Heat Generation in the Thermal Shield", DP-36.

Wesstrom, D. B., "Reactor Stresses and Deformation", DPE-772.